

Dehydrogenation of Ethene by Ti^+ and V^+ : Excited State Effects on the Mechanism for C–H Bond Activation from Kinetic Energy Release Distributions

Jennifer Gidden, Petra A. M. van Koppen,* and Michael T. Bowers*

Contribution from the Department of Chemistry, University of California, Santa Barbara, California 93106

Received December 20, 1996[⊗]

Abstract: The energetics and mechanism for dehydrogenation of ethene by early transition metals were examined. Reaction of Ti^+ and V^+ led to collision complexes that decomposed by H_2 loss on the metastable time frame (5–15 μs). Kinetic energy release distributions (KERDs) for H_2 loss were measured. Loss of H_2 from $\text{Ti}(\text{C}_2\text{H}_4)^+$ exhibited a statistical KERD with an average release (\bar{E}_t) of 0.10 eV. In contrast, $\text{V}(\text{C}_2\text{H}_4)^+$ gave a statistical release for H_2 loss at low source pressures ($\bar{E}_t = 0.021$ eV) and a strongly non-statistical release at high source pressures ($\bar{E}_t = 0.70$ eV). The two statistical releases were assigned to ground state $\text{Ti}^+(\text{4F})$ and $\text{V}^+(\text{5D})$ ions while the non-statistical release was assigned to complexes originating from the $\text{V}^+(\text{3F})$ excited state. Modeling the statistical KERDs using phase space theory yielded the bond energies, $D_0^0(\text{Ti}^+-\text{C}_2\text{H}_2) = 51 \pm 3$ kcal/mol and $D_0^0(\text{V}^+-\text{C}_2\text{H}_2) = 41 \pm 2$ kcal/mol. Why we observe two very different KERDs in the $\text{V}(\text{C}_2\text{H}_4)^+$ system at differing source pressures is discussed. The results give important information about the details of the potential energy surfaces of the two systems.

Introduction

Reactions between transition metal ions and hydrocarbons have been of particular interest to gas-phase chemical kineticists and dynamicists because of their importance in catalytic processes.¹ These reactions often involve C–H or C–C bond activation by the metal followed by elimination of hydrogen or small alkane groups.^{2–15} Recently, the primary focus has been on understanding details of the potential energy surfaces and how these relate to the factors that control σ -bond activation. Here we will consider reactions of two early first row transition metals, Ti^+ and V^+ , with the prototypical alkene, ethene.

[⊗] Abstract published in *Advance ACS Abstracts*, April 1, 1997.

(1) For reviews see: (a) Freiser, B. S., Ed. *Organometallic Ion Chemistry*; Kluwer Academic Publishers: The Netherlands, 1996. (b) Eller, K.; Schwarz, H. *Chem. Rev.* **1991**, *91*, 1121. (c) Russell, D. H., Ed. *Gas Phase Inorganic Chemistry*; Plenum: New York, 1989. (d) Allison, J. *Prog. Inorg. Chem.* **1986**

(2) (a) Armentrout, P. B. In *Gas Phase Inorganic Chemistry*; Russell, D., Ed.; Plenum: New York, 1989; p 1. (b) Armentrout, P. B. *Science* **1991**, *251*, 175. (c) Armentrout, P. B. In *Selective Hydrocarbon Activation: Principles and Progress*; Davies, J. A., Watson, P. L., Liebman, J. F., Greenberg, A., Eds.; VCH: New York, 1990; p 467.

(3) (a) Weisshaar, J. C. In *Advances in Chemical Physics*; Ng, C., Ed.; Wiley-Interscience: New York, 1992; Vol. 82, pp 213–261. (b) Weisshaar, J. C. *Acc. Chem. Res.* **1993**, *26*, 213.

(4) van Koppen, P. A. M.; Kemper, P. R.; Bowers, M. T. In *Organometallic Ion Chemistry*; Freiser, B. S., Ed.; Kluwer Academic Publishers: The Netherlands, 1996; p 157.

(5) van Koppen, P. A. M.; Kemper, P. R.; Bushnell, J. E.; Bowers, M. T. *J. Am. Chem. Soc.* **1995**, *117*, 2098.

(6) Tolbert, M. A.; Beauchamp, J. L. *J. Am. Chem. Soc.* **1986**, *108*, 7509.

(7) Aristov N.; Armentrout, P. B. *J. Am. Chem. Soc.* **1986**, *108*, 1806.

(8) Sanders, L.; Hanton, S. D.; Weisshaar, J. C. *J. Chem. Phys.* **1990**, *92*, 3498.

(9) (a) van Koppen, P. A. M.; Kemper, P. R.; Bowers, M. T. *J. Am. Chem. Soc.* **1992**, *114*, 10941. (b) van Koppen, P. A. M.; Kemper, P. R.; Bowers, M. T. *J. Am. Chem. Soc.* **1992**, *114*, 1083.

(10) Sunderlin, L. S.; Armentrout, P. B. *Int. J. Mass Spectrom. Ion Proc.* **1989**, *94*, 149.

(11) Armentrout, P. B.; Beauchamp, J. L. *J. Am. Chem. Soc.* **1981**, *103*, 784.

(12) Tonkyn, R.; Ronan, M.; Weisshaar, J. C. *J. Phys. Chem.* **1988**, *92*, 92.

(13) (a) Jacobson, D. B.; Freiser, B. S. *J. Am. Chem. Soc.* **1983**, *105*, 5197. (b) Jackson, T. C.; Carlin, T. J.; Freiser, B. S. *J. Am. Chem. Soc.* **1986**, *108*, 1120.

A previous kinetic study by Guo, Kerns, and Castleman¹⁶ indicated the reaction $\text{Ti}^+ + \text{C}_2\text{H}_4 \rightarrow \text{TiC}_2\text{H}_2^+ + \text{H}_2$ had a reaction efficiency of 30% for ground state $\text{Ti}^+(\text{4F}, 4s^1 3d^2)$ with H_2 elimination the only reaction channel. An examination of the analogous reaction between V^+ and C_2H_4 by Aristov and Armentrout⁷ also revealed dehydrogenation to be the only exothermic process. In this case, however, the reaction efficiency observed was much lower, only 0.02% at 0.05 eV collision energy. The authors argued that the reactant vanadium ion was in the ground state $\text{V}^+(\text{5D}, 3d^4)$. In state selected studies by Sanders, Hanton, and Weisshaar,⁸ the observed reaction efficiencies for dehydrogenation of ethene (at 0.2 eV collision energy) by ground state $\text{V}^+(\text{5D}, 3d^4)$ and by the low-lying excited state $\text{V}^+(\text{5F}, 3d^3 4s)$ were also low, 0.9% and 0.4%, respectively, while the reaction efficiency of V^+ in the $\text{3F}(3d^3 4s)$ excited electronic state was just over 3% even though this state lies 1.1 eV above ground state.¹⁷ Low reaction efficiencies for exothermic metal–hydrocarbon reactions are not uncommon and often indicate that the potential energy surface can be fruitfully probed and information obtained regarding the rate limiting transition state.

The mechanism proposed^{7,16} for reactions of both metals is shown in Scheme I. In this mechanism, the metal ion inserts into a C–H bond of ethene, followed by β -hydrogen migration and loss of H_2 . Also proposed⁷ is a multicenter elimination step that leads directly to products instead of a stepwise rearrangement. However, the structure of the initial collision complex and which of the proposed mechanisms is operative has not been determined.

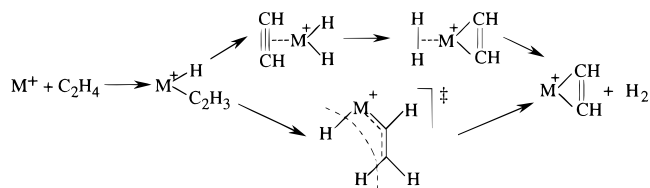
(14) (a) van Koppen, P. A. M.; Brodbelt-Lustig, J.; Bowers, M. T.; Dearden, D. V.; Beauchamp, J. L.; Fisher, E. R.; Armentrout, P. B. *J. Am. Chem. Soc.* **1991**, *113*, 2359. (b) van Koppen, P. A. M.; Brodbelt-Lustig, J.; Bowers, M. T.; Dearden, D. V.; Beauchamp, J. L.; Fisher, E. R.; Armentrout, P. B. *J. Am. Chem. Soc.* **1990**, *112*, 5663.

(15) van Koppen, P. A. M.; Bowers, M. T.; Fisher, E. R.; Armentrout, P. B. *J. Am. Chem. Soc.* **1994**, *116*, 3780.

(16) Guo, B. C.; Kerns, K. P.; Castleman, A. W., Jr. *J. Phys. Chem.* **1992**, *96*, 4879.

(17) Moore, C. E. *Atomic Energy Levels*; U.S. National Bureau of Standards: Washington, DC, 1952; circ. 467 (U.S. Natl. Bur. Stand.).

Scheme 1



Theoretical studies of the bonding between first row transition metal ions and ethene,¹⁸ as well as acetylene,¹⁹ found that both TiC_2H_4^+ and TiC_2H_2^+ are covalently bound, with ${}^2\text{A}_1$ and ${}^2\text{A}_2$ ground states, respectively, with the Ti^+ ion inserted into the π -bond in both cases. They also imply that in the reaction of ground state Ti^+ (${}^4\text{F}$) with ethene, a spin-orbit coupled crossing must occur from the quartet to the doublet surface to form TiC_2H_4^+ (${}^2\text{A}_1$). It is reasonable to assume that further reaction remains on this surface to produce TiC_2H_2^+ (${}^2\text{A}_2$) + H_2 products. Conversely, the lowest energy form of VC_2H_4^+ is the ${}^5\text{A}_1$ electrostatically bound complex. The covalently bound, ${}^3\text{A}_2$ VC_2H_4^+ excited state, with V^+ inserted into the π -bond of C_2H_4 , is about 15 kcal/mol higher in energy.¹⁸ The product ion, VC_2H_2^+ , however, is covalently bound with V^+ inserted into a π -bond of acetylene, and has a ${}^3\text{A}_2$ ground state.¹⁹ Thus, if the VC_2H_4^+ complex originates from the ${}^5\text{D}$ ground electronic state of V^+ , a spin-orbit coupled crossing from the quintet surface to the triplet surface is required to activate the C-H bond and to eliminate H_2 . On the other hand, if the VC_2H_4^+ complex originates from the ${}^3\text{F}$ electronic state of V^+ , spin is conserved in the reaction.

A number of important questions remain to be answered about these reactions. The first question concerns the difference in reactivity observed for ground state V^+ (${}^5\text{D}$) and electronically excited V^+ (${}^3\text{F}$) with ethene. Because spin is conserved for V^+ (${}^3\text{F}$) reacting with C_2H_4 to eliminate H_2 , and because the available energy is 1.1 eV greater than the corresponding ground state reaction, a much larger reaction efficiency is expected for the V^+ (${}^3\text{F}$) reaction relative to that of ground state V^+ (${}^5\text{D}$). However, both reactions are very inefficient (1% and 3%, respectively). One goal of this paper is to determine why both reactions are so inefficient.

A second question addresses the details of the potential energy surfaces. The main focus is on determining the position of the bottleneck for these reactions. In many metal-hydrocarbon reactions, a significant reaction barrier is associated with the activation of C-H bonds.^{2,3,14,15} Metal ions can often interact with neutral hydrocarbons to form chemically activated complexes with enough energy to overcome this barrier. However, if the C-H insertion transition state energy is near the asymptotic reactant energy, the reaction may still be retarded by this (or other) transition state as it proceeds along the reaction coordinate.

Another question concerns the effect of excited states on the character of the potential energy surface as well as the reaction mechanism. Previous studies have shown that the reaction surfaces originating from electronic ground and excited states of the metal ions mix.^{4,8,9,20} Thus, a ground state metal ion can react with the hydrocarbon through spin-orbit or strongly avoided crossings to produce products that correlate back to electronic excited states of the metal ion.²⁰ If, however, the reactants start in an excited state, can they follow a reaction path not available to those in the ground state?

(18) Sodupe, M.; Bauschlicher, C. W.; Langhoff, S. R.; Parttridge, H. J. *Phys. Chem.* **1992**, *96*, 2118.

(19) Sodupe, M.; Bauschlicher, C. W. *J. Phys. Chem.* **1991**, *95*, 8640.

(20) Bushnell, J. E.; Kemper, P. R.; Maitre, P.; Bowers, M. T. *J. Am. Chem. Soc.* **1994**, *116*, 9710.

The final question deals with the reaction thermochemistry. The heats of formation for the reactants and products in the $\text{M}^+ + \text{C}_2\text{H}_4 \rightarrow \text{MC}_2\text{H}_2^+ + \text{H}_2$ reaction are well established except for the MC_2H_2^+ product ion. Even though experimental^{7,10} and theoretical^{18,19} values have been reported, the discrepancy of up to 14 kcal/mol between these values is too large, well outside the experimental uncertainties reported. It is, therefore, important to obtain an independent set of experimental binding energies for comparison with theory, and to discuss the relative $\text{V}^+ - \text{C}_2\text{H}_2$ and $\text{Ti}^+ - \text{C}_2\text{H}_2$ bond energies in comparison to $\text{V}^+ - \text{C}_2\text{H}_4$ and $\text{Ti}^+ - \text{C}_2\text{H}_4$ bond energies.

To address these questions we measured KERDs for H_2 loss from $\text{V}(\text{C}_2\text{H}_4)^+$ and $\text{Ti}(\text{C}_2\text{H}_4)^+$ complexes and modeled them using statistical phase space theory.^{21,22} Measurements of this type have provided both energetic and mechanistic details for similar systems involving metal ions and hydrocarbons.^{14,15,21-23}

Experimental Section

Measurements of the metastable KERDs were obtained using a reverse geometry, double-focusing mass spectrometer (VG Instruments ZAB-2F)²⁴ with a temperature-variable ion source constructed at UCSB. The titanium and vanadium ions were formed by electron impact (200 eV) on TiCl_4 and VOCl_3 , respectively. Source pressures were varied from 10^{-4} to 10^{-3} Torr, and source temperatures were kept at 300 K.

The populations of the principal electronic states of V^+ and Ti^+ formed by electron impact on VOCl_3 and TiCl_4 , respectively, have been determined using the ion chromatography technique.²⁵ In this technique the mobilities of atomic transition metal ions in He can be used to separate electronic states with different electron configurations ($3d^n$ and $4s^1 3d^{n-1}$) and, in many cases, the low and high spin states within the $4s^1 3d^{n-1}$ electron configuration. The arrival time distribution (ATD) for V^+ in He is shown in Figure 1. The three resolved features correspond to $3d^4$ and $4s^1 3d^3$ (low and high spin) electronic configurations of V^+ . In recent pressure dependent studies of V^+ ATDs in He,²⁶ both low- and high-spin $4s^1 3d^{n-1}$ configurations were observed in 2 Torr of He but only the high-spin configuration was observed in 8 Torr of He. At intermediate pressures, a decrease in the low- to high-spin ratio was observed with increasing pressure, clearly indicating deactivation of the low-spin to the high-spin configuration. The ${}^3\text{F}, 4s^1 3d^3$ and ${}^5\text{F}, 4s^1 3d^3$ states were, therefore, assigned as shown in Figure 1. The high-spin ${}^5\text{F}, 4s^1 3d^3$ state did not, however, deactivate to the ${}^5\text{D}, 3d^4$ ground state in He at thermal energies. It is important to note that in the ATD experiments, the VOCl_3 pressure in the source was on the order of 10^{-4} to 10^{-3} Torr. This is exactly the range in total source pressure of VOCl_3 and C_2H_4 used in our experiments to measure the KERDs for H_2 loss from $\text{V}(\text{C}_2\text{H}_4)^+$. Thus, the electronic state distribution shown in Figure 1 is a good representation of the electronic state distribution in the present experiments. In the ATD of Ti^+ in He, three $4s^1 3d^{n-1}$ states are resolved with $45 \pm 3\%$ assigned to the ${}^4\text{F}, 4s^1 3d^2$ ground state of Ti^+ for electron energies ≥ 50 eV.²⁵ The low-lying first excited state of Ti^+ ${}^4\text{F}, 3d^3$ is not observed in the chromatography experiments²⁵ and, therefore, cannot contribute to the KERD for H_2 loss from $\text{Ti}(\text{C}_2\text{H}_4)^+$.

The organometallic ions were formed in the ion source by the reaction of the bare metal ions with neutral ethene. After exiting the

(21) (a) Hanratty, M. A.; Beauchamp, J. L.; Illies, A. J.; Bowers, M. T. *J. Am. Chem. Soc.* **1985**, *107*, 1788. (b) Hanratty, M. A.; Beauchamp, J. L.; Illies, A. J.; vanKoppen, P. A. M.; Bowers, M. T. *J. Am. Chem. Soc.* **1988**, *110*, 1.

(22) (a) vanKoppen, P. A. M.; Jacobson, D. B.; Illies, A. J.; Bowers, M. T.; Hanratty, M. A.; Beauchamp, J. L. *J. Am. Chem. Soc.* **1989**, *111*, 1991. (b) vanKoppen, P. A. M.; Bowers, M. T.; Beauchamp, J. L. *Organometallics* **1990**, *9*, 625.

(23) van Koppen, P. A. M.; Jacobson, D. B.; Illies, A.; Bowers, M. T.; Hanratty, M.; Beauchamp, J. L. *J. Am. Chem. Soc.* **1989**, *111*, 1991.

(24) Morgan, R. P.; Beynon, J. H.; Bateman, R. H.; Green, B. N. *Int. J. Mass Spectrom. Ion Proc.* **1978**, *28*, 171.

(25) (a) Kemper, P. R.; Bowers, M. T. *J. Phys. Chem.* **1991**, *95*, 5134. (b) For a general discussion see: Bowers, M. T.; Kemper, P. R.; von Helden, G.; van Koppen, P. A. M. *Science* **1993**, *260*, 1446 or ref 4.

(26) Weis, P.; Kemper, P.; Bowers, M. T. To be submitted for publication.

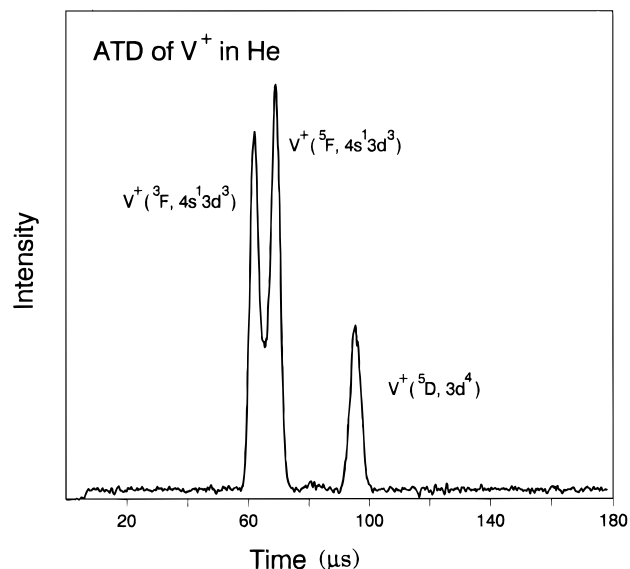


Figure 1. Arrival time distribution (ATD) of V^+ formed by electron impact (EI) on $VOCl_3$ at 180 eV. A broad distribution of electronic states can be formed by EI. While each of the three resolved features in the figure can be assigned to specific electronic configurations, each configuration could include higher lying electronic states as well. The populations of the principal electronic states of V^+ formed by EI have been published (ref 25).

source, the ions were accelerated to 8 kV and mass analyzed with the magnetic sector. Metastable ions decomposing in the second field free region between the magnetic and electric sectors were energy analyzed by scanning the voltage of the electric sector. The metastable peaks were collected with a multichannel analyzer and differentiated to yield kinetic energy release distributions.²⁷ The reported KERDs represent an average of several hundred scans repeated on at least two separate occasions. The error bars on the bond energies reported, $D_0^0(Ti^+-C_2H_2) = 51 \pm 3$ kcal/mol and $D_0^0(V^+-C_2H_2) = 41 \pm 2$ kcal/mol, are arrived at by varying these values and comparing model KERDs with experiment. These are conservative estimates as "reasonable" fits were not obtained when the maximum deviations in the bond energies were utilized. The error in the bond energies is less for V^+ than for Ti^+ because H_2 loss from $V(C_2H_4)^+$ is very nearly thermoneutral and is, therefore, more sensitive to the available energy of reaction.

All compounds were obtained commercially and introduced into the mass spectrometer after several freeze-pump-thaw cycles to remove non-condensable gases.

Results

The experimental kinetic energy release distributions (KERDs) for elimination of H_2 are shown in Figures 2 and 3. Two distinctly different results are observed for V^+ . When the $VC_2H_4^+$ adduct was formed at relatively low source pressures (8×10^{-4} Torr), the observed KERD appears statistical with the peak maximum located near zero center of mass kinetic energy and drops off smoothly with increasing energy (Figure 2a). The average kinetic energy release for this reaction is 0.021 eV. When the adduct was formed at higher source pressures (5×10^{-3} Torr), the KERD is much broader and appears to be non-statistical (Figure 2b). In this case the peak maximum is shifted to higher energies and the average kinetic energy release is 0.70 eV, which is over 30 times greater than the average release observed at lower pressure.

Only one KERD for H_2 loss is observed for Ti^+ reacting with C_2H_4 , independent of the source pressure (Figure 3). It appears statistical and has an average kinetic energy release of 0.17 eV.

(27) (a) Jarrold, M. F.; Illies, A. J.; Bowers, M. T. *Chem. Phys.* **1982**, 65, 19. (b) Kirchner, N. J.; Bowers, M. T. *J. Phys. Chem.* **1987**, 91, 2573.

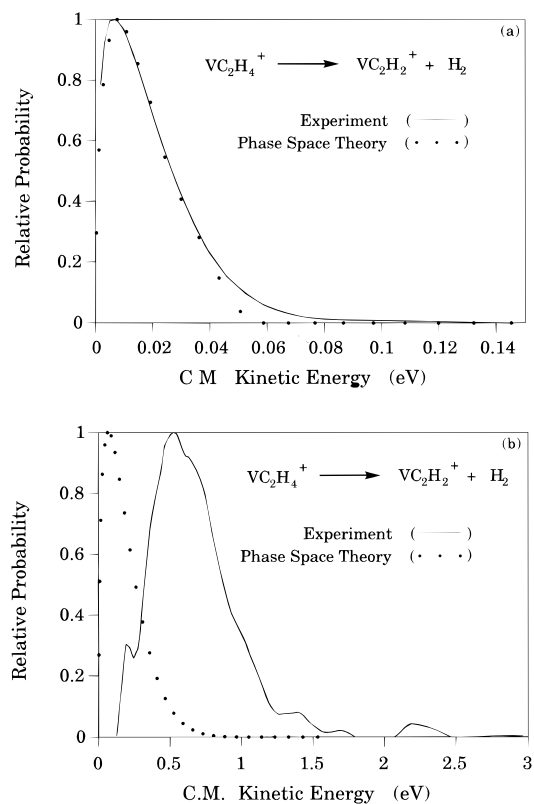


Figure 2. Kinetic energy release distribution (KERD) for H_2 loss from metastable $V(C_2H_4)^+$ collision complexes formed at (a) low source pressure (8×10^{-4} Torr) and (b) high source pressure (5×10^{-3} Torr). The experimental KERD (solid line) is obtained by differentiating the laboratory peak. The dotted lines result from statistical phase space calculations for the $V^+(^5D)$ ground state (Figure 1a) and the $V^+(^3F)$ electronically excited state (Figure 1b). Note the energy scale is significantly different in the two figures.

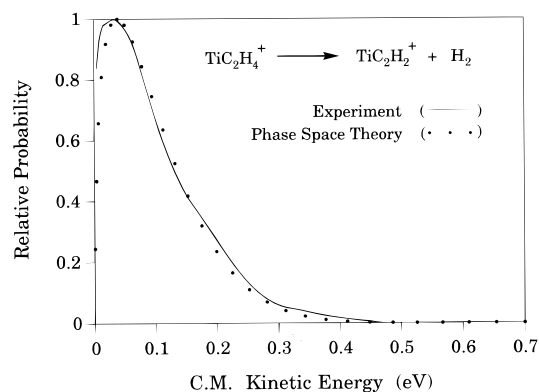


Figure 3. KERD for H_2 loss from metastable $Ti(C_2H_4)^+$ collision complexes. The experimental KERD (solid line) is obtained by differentiating the laboratory peak. The dotted line results from statistical phase space calculations for the $Ti^+(^4F)$ ground state.

Phase space theory is used to model the experimental KERDs.^{28,29} The resulting theoretical KERDs are shown in comparison with the experimental KERDs in Figures 2 and 3. The main purpose of the calculation is to determine whether a statistical model, which assumes a potential energy surface without a reverse activation energy barrier, can accurately describe the experimental results. The only variable parameter

(28) (a) Pechukas, P.; Light, J. C.; Rankin, C. *J. Chem. Phys.* **1966**, 44, 794. (b) Nikitin, E. *Theor. Exp. Chem. (Engl. Transl.)* **1965**, 1, 285.

(29) (a) Chesnavich, W. J.; Bowers, M. T. *J. Am. Chem. Soc.* **1976**, 98, 8301. (b) Chesnavich, W. J.; Bowers, M. T. *J. Chem. Phys.* **1978**, 68, 901. (c) Chesnavich, W. J.; Bowers, M. T. *Prog. React. Kinet.* **1982**, 11, 137.

Table 1. Reaction Enthalpies and Average Kinetic Energy Releases from Experiment and Phase Space Theory

reaction	$-\Delta H$ (eV) ^a	\bar{E}_i (eV)	
		expt	theory ^b
$V^+ + C_2H_4 \rightarrow VC_2H_2^+ + H_2$	0.05 ^c	0.02 ^c	0.02
$Ti^+ + C_2H_4 \rightarrow TiC_2H_2^+ + H_2$	0.45	0.10	0.10

^a Heat of reaction at 0 K. ^b Statistical phase space theory using the methods outlined in refs 28 and 29. ^c Low pressure in the ion source (8×10^{-4} Torr). ^d High pressure in the ion source (5×10^{-3} Torr). ^e Actual value is 1.3 kcal/mol or 0.055 eV.

used in these calculations is the heat of reaction. All of the parameters used in the calculations are summarized in the Appendix. For V^+ , only the experimental KERD obtained under low-pressure conditions could be modeled successfully yielding $\Delta H_{rxn} = -1.3$ kcal/mol, corresponding to a $V^+-C_2H_2$ bond energy of 41 ± 2 kcal/mol. For Ti^+ , theoretical modeling of the experimental KERD results in $\Delta H_{rxn} = -10.4$ kcal/mol, corresponding to a $Ti^+-C_2H_2$ bond energy of 51 ± 3 kcal/mol. The results are summarized in Table 1.

Discussion

A. Vanadium. For V^+ reacting with ethene we determined that dehydrogenation is exoergic by 1.3 kcal/mol. The shape of the energy dependent cross section⁷ for ground state V^+ reacting with C_2H_4 confirms the reaction is exoergic and indicates that no barriers along the reaction coordinate exceed the asymptotic energy of the reactants. The observed inefficiency of this reaction is, therefore, due to a rate limiting transition state along the reaction coordinate with an energy near the reactant energy.

The KERD for H_2 loss obtained when $VC_2H_4^+$ is formed at relatively low source pressure is clearly statistical (Figure 1a). The good agreement between theory and experiment, assuming 100% ground state V^+ reacting with C_2H_4 , indicates that there is no significant reverse activation barrier in the exit channel (in agreement with the cross section measurements⁷) and that the KERD is primarily due to $V(C_2H_4)^+$ complexes formed from ground state V^+ . The contribution of the 5F , first excited state of V^+ toward the very narrow H_2 loss KERD must be insignificant for the following reasons. First, the reaction efficiency at 0.2 eV collision energy is only 0.4% for the 5F state,⁸ which is less than half that of ground state V^+ . At thermal energy the reaction efficiency of the 5F state relative to the 5D state may be even lower. Second, the available energy for the excited state reaction is over a factor of 6 times greater than for the ground state reaction. Hence, a bimodal distribution would be expected if both ground and excited state V^+ were contributing to the KERD.

The H_2 loss KERD obtained when $VC_2H_4^+$ is formed at a higher source pressure cannot be modeled successfully using phase space theory. The average kinetic energy release (0.7 eV) for this reaction is much higher than the total amount of energy available (0.06 eV) for the ground state reaction. Therefore, this second reaction cannot be from V^+ ions in their ground state. An excited state reaction is possible since the ion chromatography results (Figure 1) indicate that V^+ ions are formed in the $^5D, 3d^4$ ground state, as well as the 5F and $^3F, 4s^1 3d^3$ excited states, under our experimental conditions. Because the available energy for the 3F reaction is on the order of 1.2 eV and dehydrogenates C_2H_4 with a low enough efficiency (only 3%)⁸ to allow metastable decomposition to be observed in our experimental time window, the 3F excited state of V^+ is a likely candidate for this reaction. The KERD for H_2 loss is clearly

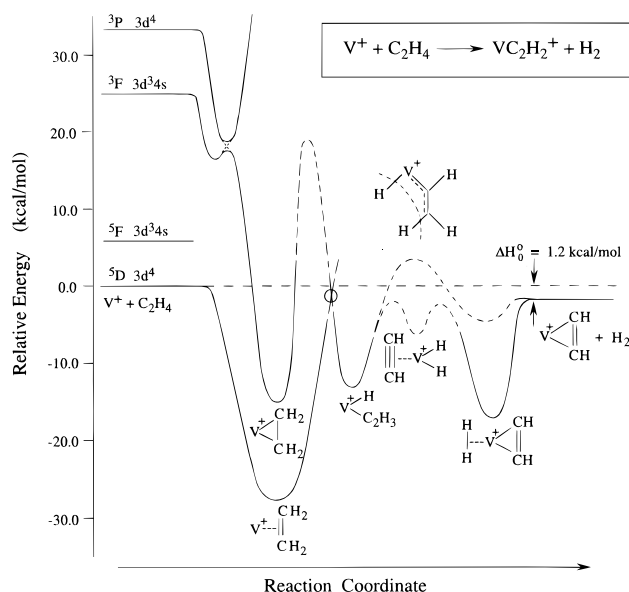


Figure 4. Schematic reaction coordinate diagram for the reaction of $V^+(^5D)$ and $V^+(^3F)$ with ethene to eliminate H_2 . The energies of the electrostatic and covalently bound $V(C_2H_4)^+$ complexes were calculated using ab initio methods.^{18,29} The overall reaction exothermicity was determined in this study by modeling the experimental H_2 loss KERD using statistical phase space theory. Energies of the remaining intermediates were estimated. For example, the inserted $(H)V^+(C_2H_3)$ intermediate was estimated from V^+-H , V^+-CH_3 , and $CH_3V^+-CH_3$ bond energies (see bond energy table in ref 1a).

non-statistical for this excited state reaction (Figure 2b). Because the peak of the experimental H_2 loss KERD is shifted significantly away from zero energy, dissociation occurs much faster than the time necessary for energy randomization, suggesting a reverse activation energy barrier along this reaction coordinate.

A schematic reaction coordinate diagram for the dehydrogenation of ethene by ground and excited state V^+ ions, consistent with the experimental results, is shown in Figure 4. Ground state $V^+(^5D)$ reacts with ethene to initially form the electrostatically bound 5A_1 $VC_2H_4^+$ complex.¹⁸ C–H bond activation requires a spin–orbit coupled crossing from the quintet to the triplet surface to form the $H-V^+-C_2H_3$ inserted intermediate. Because the overall reaction is only slightly exothermic (1.3 kcal/mol), the energy of the rate limiting transition state must be near the reactant energy as well. At this point it is not clear where the bottleneck lies. It could be the spin–orbit coupled crossing, β -H migration, or H–H coupling. In fact, the energy difference between these transition states could be minimal.

In contrast to the ground state V^+/C_2H_4 reaction, excited state $V^+(^3F)$ reacts with ethene to initially form the covalently bound 3A_2 $VC_2H_4^+$ complex, which is approximately 15 kcal/mol higher in energy than the electrostatically bound 5A_1 $VC_2H_4^+$ complex.¹⁸ The reaction stays on the triplet surface to form the $H-V^+-C_2H_3$ intermediate and to eliminate H_2 to form the triplet $VC_2H_2^+$ product ion. Once the $H-V^+-C_2H_3$ intermediate is formed, the low-energy pathway followed by the ground state V^+/C_2H_4 reaction is available. Thus, the rate limiting transition state must occur prior to $H-V^+-C_2H_3$ formation, indicating C–H bond activation must be the bottleneck in this reaction. To account for the low reaction efficiency observed,⁸ the barrier height from the bottom of the 3A_2 $VC_2H_4^+$ well would need to be about 25–30 kcal/mol, which is reasonable for C–H bond activation.^{4,14,15} The high-energy non-statistical experimental KERD indicates that once the rate limiting transition state is passed, the reaction proceeds very quickly.

Scheme 2

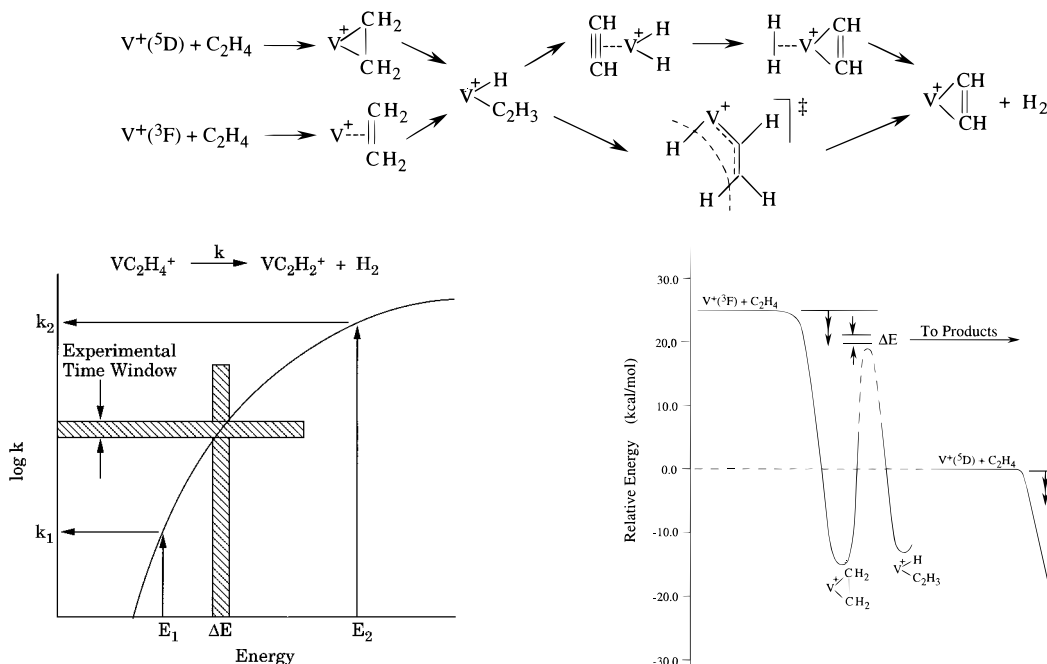


Figure 5. A plot of $\log k$ versus the internal energy of the $V(C_2H_4)^+$ collision complex. For $V(C_2H_4)^+$ complexes with internal energy in the range ΔE , the dissociation rates fall within the experimental time window.

At this point the reaction could follow that of ground state V^+/C_2H_4 or proceed via a multicenter transition state to eliminate H_2 . These results are summarized in the proposed mechanism shown in Scheme 2.

The observed pressure dependence of the KERDs can be rationalized in the following way. A schematic plot of $\log k$ versus energy is shown in Figure 5. In our experiment the observation time window is 5–15 μs . $VC_2H_4^+$ ions with an energy range ΔE will decompose in this time window (Figure 5). The appropriate ΔE values for ground and excited state V^+ ions are schematically shown in Figure 6. To a good approximation if $VC_2H_4^+$ has an energy E_1 which is less than ΔE , the dissociation will be too slow and products will not be observed. If $VC_2H_4^+$ has an energy E_2 that is greater than ΔE , the dissociation will be too fast and products will not be observed. As the pressure inside the ion source increases, the time between collisions decreases and the probability the nascent $(V^+/C_2H_4)^*$ complex undergoes a collision increases. Consequently, complexes of ground state $V^+(\text{}^5D)$ with C_2H_4 are collisionally stabilized since the transition state must be very near the $V^+(\text{}^5D)/C_2H_4$ asymptotic energy. These same collisions can help bring excited state $V^+(\text{}^3F)/C_2H_4$ complexes into the energy range required for metastable decomposition (see Figure 6). In contrast, at low source pressure, the unquenched excited state $V^+(\text{}^3F)/C_2H_4$ complexes will be too high in energy, reacting away prior to our experimental time window, while the ground state $V^+(\text{}^5D)/C_2H_4$ complexes dissociate within our experimental time window (Figure 6). As a result, the KERD measured at low pressure appears to be due exclusively to dissociation of nascent ground state $V^+(\text{}^5D)/C_2H_4$ complexes, while at higher source pressure the KERD appears to be only due to dissociation of partially collisionally stabilized excited state $V^+(\text{}^3F)/C_2H_4$ complexes.

We tried very hard to detect both processes simultaneously at intermediate pressures but were unsuccessful. The reason is that every collision stabilizes ground state reactants below the dissociation threshold while it appears to take more than one

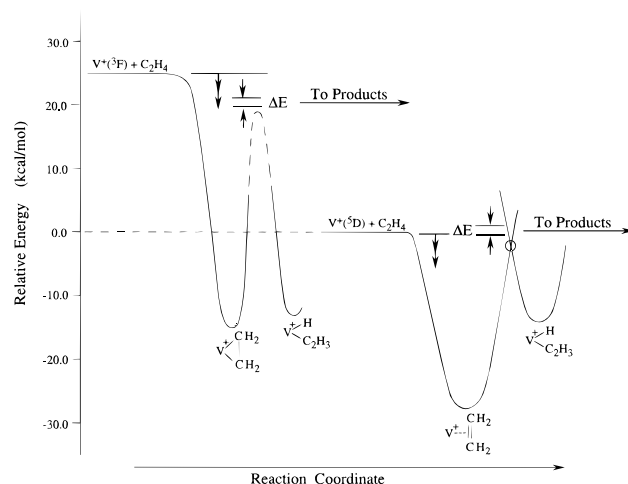


Figure 6. Schematic reaction coordinate diagram for the reaction of $V^+(\text{}^5D)$ and $V^+(\text{}^3F)$ with ethene to eliminate H_2 . Only $V(C_2H_4)^+$ complexes within the energy range ΔE will dissociate within the experimental time window. Collisional deactivation of the $V^+(\text{}^3F)/C_2H_4$ complex is necessary to lower the energy of the complex to within the energy range, ΔE , and to observe H_2 loss in the experimental time window. For the ground state $V^+(\text{}^5D)/C_2H_4$ complex, all collisions deactivate the complex and hence only nascent $V^+(\text{}^5D)/C_2H_4$ collision complexes will dissociate in the experimental time window.

collision to access the experimental time window for $V^+(\text{}^3F)/C_2H_4$ complexes.

B. Titanium. For Ti^+ reacting with C_2H_4 , analysis of the KERD indicates H_2 loss is exothermic by 10.4 kcal/mol. The reaction efficiency of 30%¹⁶ indicates a rate limiting transition state somewhere along the reaction coordinate with an energy significantly below (5–10 kcal/mol) the reactant energy.

The KERD for H_2 loss from $TiC_2H_4^+$ is clearly statistical (Figure 2). The experimental KERD can be fit very well with statistical phase space theory assuming 100% of the Ti^+ ions are in the $4F(3d^24s)$ ground electronic state. The agreement between theory and experiment indicates that there is no significant reverse activation barrier in the region of the exit channel and that the reaction is due to ground state Ti^+ .

A schematic reaction coordinate diagram for ground state Ti^+ reacting with C_2H_4 consistent with the experimental results is shown in Figure 7. The mixing of ground and excited electronic states of Ti^+ is apparent. Ground state $Ti^+(\text{}^4F)$ reacts with ethene to initially form the electrostatically bound ${}^4B_2 TiC_2H_4^+$ adduct. A spin-orbit coupled crossing from the quartet surface to the doublet surface is required to form the covalently bound ${}^2A_1 TiC_2H_4^+$ complex, which is calculated to be ~ 5 kcal/mol lower in energy than the 4B_2 complex.¹⁸ The remainder of the reaction takes place on the doublet surface. C–H bond activation is energetically feasible for ground state Ti^+/C_2H_4 reactants even if it requires on the order of 25–30 kcal/mol from the bottom of the ${}^2A_1 TiC_2H_4^+$ well. From our data it is not clear which transition state is rate limiting for H_2 elimination. In analogy with the $V^+(\text{}^3F)/C_2H_4$ reaction, C–H bond activation may be rate limiting for the Ti^+/C_2H_4 reaction but we cannot

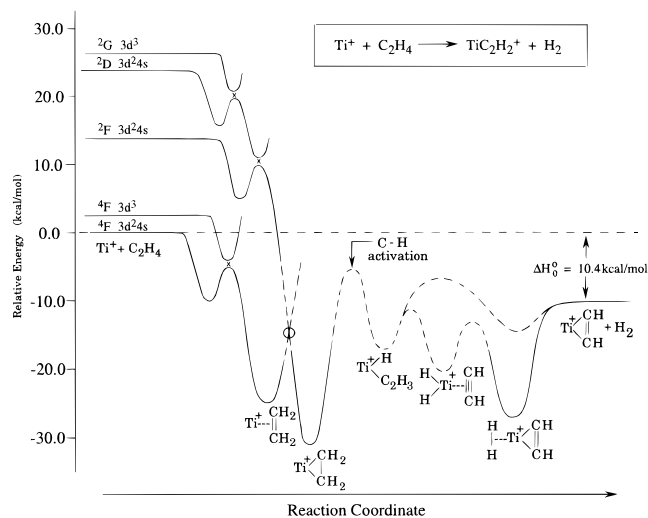


Figure 7. Schematic reaction coordinate diagram for the reaction of $\text{Ti}^+(\text{4F})$ with ethene to eliminate H_2 . The effect of electronically excited states of Ti^+ on the ground state $\text{Ti}^+/\text{C}_2\text{H}_4$ reaction is shown. The energies of the electrostatic and covalently bound $\text{Ti}(\text{C}_2\text{H}_4)^+$ complexes were calculated using ab initio methods.^{18,29} The overall reaction exothermicity was determined in this study by modeling the experimental H_2 loss KERD using statistical phase space theory. Energies of the remaining intermediates were estimated. For example, the inserted $(\text{H})\text{Ti}^+(\text{C}_2\text{H}_3)$ intermediate was estimated from Ti^+-H , Ti^+-CH_3 , and $\text{CH}_3\text{Ti}^+-\text{CH}_3$ bond energies (see bond energy table in ref 1a).

rule out β -H transfer, H-H coupling, or a multicenter transition state as the rate limiting transition state to eliminate H_2 .

C. Thermochemistry. The $\text{V}^+-\text{C}_2\text{H}_2$ and $\text{Ti}^+-\text{C}_2\text{H}_2$ bond energies of 41 ± 2 and 51 ± 3 kcal/mol, respectively, obtained by modeling the experimental KERD using statistical phase space theory, are in good agreement with the relative bond energies of 35 and 47 kcal/mol calculated using ab initio methods.^{18,19} Previously reported experimental bond energies of 48.9 ± 4.6 ^{7,30} and 60.4 ± 4.6 kcal/mol^{10,30} for $\text{V}^+-\text{C}_2\text{H}_2$ and $\text{Ti}^+-\text{C}_2\text{H}_2$, respectively, appear to be too high, somewhat outside of the error bars of the two experiments. The relative values, however, are in good agreement in all cases, indicating a stronger $\text{Ti}^+-\text{C}_2\text{H}_2$ bond energy relative to $\text{V}^+-\text{C}_2\text{H}_2$ by 10 kcal/mol.

Calculating M^+-L binding energies for an entire transition metal row often explains the trends in bond energies observed experimentally. For example, in calculating $\text{M}^+-\text{C}_2\text{H}_2$ and $\text{M}^+-\text{C}_2\text{H}_4$ bond energies for first row transition metal ions, several factors were shown to influence the bond energy.^{18,19,31} First, the promotion energy from the ground electronic configuration of the bare metal ion to an excited electron configuration in which the metal ion is covalently bound to a ligand is an important consideration.³¹ The promotion energy has been shown to correlate directly to M^+-L bond energies.³² Second, the loss in dd-electron exchange energy can significantly

Table 2. Theoretical and Experimental Bond Energies^a for MC_2H_2^+ , MC_2H_4^+ , and MC_3H_6^+

metal	bonding	MC_2H_2^+		MC_2H_4^+	MC_3H_6^+
		theory ^b	expt ^c	theory ^b	expt ^d
Ti	covalent	47	51 ± 3	31	34.5 ± 3
	electrostatic	26		23	
V	covalent	35	41 ± 2	18	
	electrostatic	29		29	30.7 ± 3

^a In kcal/mol. ^b References 18 and 19. ^c This work. ^d Reference 34. MC_2H_4^+ bond energies are expected to be slightly lower than MC_3H_6^+ in line with the theoretical MC_2H_4^+ bond energies.

decrease bond strengths.³¹ This is important especially for the less than half-filled d-shell atomic metal ions such as the ^5D , d^4 ground state of V^+ . Third, it was shown that sd hybridization is more favorable for the early transition metals than for the late transition metals because the radial extent of the s and d orbitals is more comparable for the early metals.³¹ As a result, covalent bonding is favorable for Sc^+ and Ti^+ but becomes less favorable for V^+ , Cr^+ , and the later transition metal ions. Conversely, radial contraction across the row increases the electrostatic bond strength for the later transition metal ions.³¹ V^+ is caught in the middle, binding electrostatically to ethene and covalently to acetylene (primarily due to the weaker π -bond of acetylene relative to that of ethene, by 28 kcal/mol), whereas Ti^+ binds covalently to both ethene and acetylene. The theoretical bond energies in comparison with the experimental bond energies for MC_2H_2^+ and MC_2H_4^+ are summarized in Table 2. The switch from covalent bonding being energetically favorable for VC_2H_2^+ to electrostatic bonding being energetically favorable for VC_2H_4^+ predicted theoretically is reproduced experimentally. Even though no experimental bond energies have been determined for $\text{M}^+(\text{ethene})$, the $\text{M}^+(\text{propene})$ bond energies should be very similar to $\text{M}^+(\text{ethene})$ and are, therefore, used to compare with the theoretical MC_2H_4^+ bond energies. It is also important to note that the covalently bound TiC_2H_2^+ binds 21 kcal/mol stronger than the electrostatically bound TiC_2H_2^+ , whereas for VC_2H_2^+ this difference is only 6 kcal/mol, again indicating that the formation of covalent bonds is less favorable for V^+ than for Ti^+ . These effects are shown to be important in the relative reactivity of Ti^+ and V^+ with C_2H_4 discussed in the following section.

D. Relative Reactivity of Ti^+ and V^+ with C_2H_4 . Dehydrogenation of ethene appears to be better facilitated by Ti^+ than V^+ . This is experimentally observed in the higher reaction efficiency for ground state Ti^+ of 30%¹⁶ compared to 1%^{7,8} for ground state V^+ and 3% for the ^3F electronically excited state of V^+ .⁸ The main reason for this difference is that Ti^+ forms stronger covalent bonds than V^+ . The energetics for the reactants, intermediates, and products are shown in the schematic reaction coordinate diagrams for V^+ and Ti^+ dehydrogenating ethene, in Figures 4 and 7. The difference in bonding between VC_2H_4^+ and TiC_2H_4^+ is shown to affect both the mechanism and the efficiency for dehydrogenation. Because ground state V^+ reacts with ethene to form the electrostatic VC_2H_4^+ complex, a spin-orbit coupled crossing from the quintet to the triplet surface must occur to activate the C-H bond and to eliminate H_2 . This reaction is very nearly thermoneutral, and the energies of transition states along the reaction coordinate, such as C-H bond activation, β -H transfer, or H-H coupling, are likely to be near threshold energy for reaction, giving rise to the reaction inefficiency. In contrast, the ^3F electronically excited state of V^+ as well as ground state Ti^+ both react with ethene to form a covalently bound MC_2H_4^+ complex and spin is conserved to eliminate H_2 . Both ground state Ti^+ and the ^3F state of V^+ must overcome the C-H bond activation energy barrier.

(30) Armentrout, P. B. In *Organometallic Ion Chemistry*; Freiser, B. S., Ed.; Kluwer Academic Publishers: The Netherlands, 1996; p 1.

(31) Bauschlicher, C. W.; Langhoff, S. R.; Partridge, H. In *Organometallic Ion Chemistry*; Freiser, B. S., Ed.; Kluwer Academic Publishers: The Netherlands, 1996; p 47.

(32) Armentrout, P. B. In *Bonding Energetics in Organometallic Compounds*; Marks, T. J., Ed.; ACS Symposium Series 428; American Chemical Society: Washington, DC, 1990; p 18.

(33) (a) Shimanouchi, T. *Table of Molecular Vibrational Frequencies*; National Bureau of Standards: Washington, DC, 1972; Consolidated, Vol. I. (b) Sverdlov, L. M.; Kovner, M. A.; Krainov, E. P. *Vibrational Spectra of Polyatomic Molecules*; Wiley: New York, 1970.

(34) van Koppen, P. A. M.; Bowers, M. T.; Haynes, C.; Armentrout, P. B. Manuscript in preparation.

Table 3. Input Parameters Used in Calculations

	V^+	Ti^+	C_2H_4	$V^+-C_2H_4$	$Ti^+-C_2H_4$	$Ti^+-C_2H_2$	$V^+-C_2H_2$	H_2
$\Delta H_{f,0}^{a,d}$	278	269	14.515			267 ^f	291 ^f	0
B^b	0.398	0.404	1.588					60.86
σ^c			4	1	1	4	4	2
α^d			4.26					0.808
ν_1^e			3026	3026	3026	3374	3374	4395
			1623	1623	1623	1974	1974	
			1342	1342	1342	3289	3289	
			1023	1023	1023	612(2)	612(2)	
			3103	3103	3103	730(2)	730(2)	
			1236	1236	1236	300	300	
			949	949	949	250	250	
			943	943	943	200	200	
			3106	826	826			
			826	2989	2989			
			2989	1444	1444			
			1444	350	350			
				300	300			
				250	250			

^a Heat of formation at 0 K in kcal mol⁻¹. ^b Rotational constants in cm⁻¹. ^c Symmetry number. ^d Polarizability in Å³. ^e Vibrational frequencies in cm⁻¹. ^f Determined in this study.

Because the covalently bound $TiC_2H_4^+$ complex, $(H)Ti^+(C_2H_3)$ inserted intermediate, and the $TiC_2H_2^+$ product ion are all lower in energy relative to the ground state $Ti^+(^4F)/C_2H_4$ asymptote than the corresponding V^+ species (on the triplet surface), the entire reaction surface is shifted to lower energies for Ti^+ , resulting in a lower C–H bond activation transition state energy and a greater reaction efficiency for Ti^+ compared to $^3F V^+$.

Conclusion

By measuring KERDs for H_2 loss from $V(C_2H_4)^+$ and $Ti(C_2H_4)^+$ complexes and modeling these using statistical phase space theory,^{21,22} we can draw the following conclusions.

(1) The KERDs for dehydrogenation of ethene by both ground state $V^+(^5D)$ and ground state $Ti^+(^4F)$ are statistical. Theoretical modeling of the KERDs yields $\Delta H_{rxn} = -1.3$ kcal/mol for $V^+(^5D)$ and $\Delta H_{rxn} = -10.4$ kcal/mol for $Ti^+(^4F)$, corresponding to the bond energies $D_0^0(V^+-C_2H_2) = 41$ kcal/mol and $D_0^0(Ti^+-C_2H_2) = 51$ kcal/mol. These results are in good agreement with the bond energies calculated for the covalently bound $VC_2H_2^+(^3A_2)$ and $TiC_2H_2^+(^2A_2)$ species, 35¹⁹ and 47 kcal/mol,¹⁹ respectively, indicating both V^+ and Ti^+ insert into the π -bond of acetylene.

(2) Activating a C–H bond of ethene to form the inserted $H-M^+-C_2H_3$ intermediate involves both ground and excited electronic states of V^+ and Ti^+ . The $H-M^+-C_2H_3$ intermediates correlate to a component of electronically excited, low-spin, $3d^n$ states which are 1.45 and 1.12 eV above ground state $V^+(^5D)$ and ground state $Ti^+(^4F)$, respectively. Even so, both V^+ and Ti^+ , in their ground electronic states, are observed to dehydrogenate ethene, each with a unique mechanism. $Ti^+(^4F)$ reacts with ethene via a spin–orbit coupled crossing to form the covalently bound $TiC_2H_4^+(^2A_1)$ complex and conserves spin to activate a C–H bond, forming the doublet $H-Ti^+-C_2H_3$ intermediate, which subsequently forms the $TiC_2H_2^+(^2A_2) + H_2$ products. In contrast, $V^+(^5D)$ reacts with ethene to form an

electrostatically bound $VC_2H_4^+(^5A_1)$ complex followed by a spin–orbit coupled crossing to form the triplet inserted $H-V^+-C_2H_3$ intermediate, and spin is conserved to form the products, $VC_2H_2^+(^3A_2) + H_2$.

(3) The non-statistical KERD observed for the dehydrogenation of ethene by excited state $V^+(^3F)$ is due to an energy barrier associated with C–H bond activation, consistent with the inefficiency (3%) observed for this reaction.⁸ Even though the reaction of $V^+(^3F)$ with ethene is similar to the ground state $Ti^+(^4F)/C_2H_4$ reaction (in that they both form covalently bound $MC_2H_4^+$ complexes and both conserve spin to activate the C–H bond and to eliminate H_2) the V^+ reaction is much less efficient than that of Ti^+ because V^+ forms weaker covalent bonds than Ti^+ .

Acknowledgment. The support of the National Science Foundation under grant CHE-9421176 is gratefully acknowledged. We also thank Dr. Paul Kemper and Dr. Patrick Weiss for providing the V^+ arrival time distribution.

Appendix

The model for statistical phase space calculations has been previously outlined.^{14,15,21,22} The parameters used in the calculations are summarized in Table 3.

Structures and vibrational frequencies of the various species are required for calculating KERDs. These were taken from the literature when possible, or estimated from literature values of similar species.³¹ The KERDs were strongly dependent on the total energy available to the complex but only weakly dependent on the structure and vibrational frequencies. The heats of formation of the $MC_2H_2^+$ product were used as variables in the calculation by fitting the experimental KERDs with the theoretical distributions.

JA964377+